Paper-Based Microfluidic Electrochemical Immunodevice Integrated with Nanobioprobes onto Graphene Film for Ultrasensitive Multiplexed Detection of Cancer Biomarkers

ARTICLE *in* ANALYTICAL CHEMISTRY · AUGUST 2013

Impact Factor: 5.64 · DOI: 10.1021/ac401445a · Source: PubMed

4 AUTHORS, INCLUDING:

Yuejun Kang
Southwest University, Chongqing, China
101 PUBLICATIONS **1,221** CITATIONS

analytical chemistry

Article

pubs.acs.org/ac

Paper-Based Microfluidic Electrochemical Immunodevice Integrated with Nanobioprobes onto Graphene Film for Ultrasensitive Multiplexed Detection of Cancer Biomarkers

Yafeng Wu,[†] Peng Xue,[†] Yuejun Kang,*[,†] and Kam M. Hui*[,‡,§,⊥]

[†]School of Chemical and Biomedical Engineering, Nanyang Technological University, 62 Nanyang Drive, Singapore, 637459

[‡]Division of Cellular and Molecular Research, National Cancer Center, 11 Hospital Drive, Singapore 169610

[§]Department of Biochemistry, Yong Loo Lin School of Medicine, National University of Singapore, Singapore 119228

[⊥]Program in Cancer and Stem Cell Biology, Duke-NUS Graduate Medical School, Singapore 169857

Supporting Information

ABSTRACT: To the best of our knowledge, this was the first report on the integration of a signal amplification strategy into a microfluidic paper-based electrochemical immunodevice for the multiplexed measurement of cancer biomarkers. Signal amplification was achieved through the use of graphene to modify the immunodevice surface to accelerate the electron transfer and the use of silica nanoparticles as a tracing tag to label the signal antibodies. Accurate, rapid, simple, and inexpensive point-of-care electrochemical immunoassays were demonstrated using a photoresist-patterned microfluidic paper-based analytical device (μPAD). Using the horseradish peroxidase (HRP)−*O*-phenylenediamine−H_2O_2 electrochemical detection system, the potential clinical applicability of this immunodevice was demonstrated through its ability to identify four candidate cancer biomarkers in serum samples from cancer patients. The novel signal-amplified strategy proposed in this report greatly enhanced the sensitivity of the detection of cancer biomarkers. In addition, the electrochemical immunodevice exhibited good stability, reproducibility, and accuracy and thus had potential applications in clinical diagnostics.

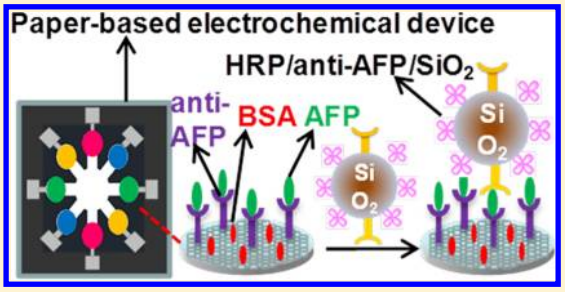

Microfluidic paper-based analytical devices (μPADs) have attracted increasing attention and interest during recent years.[1−5] These systems combine the simplicity, portability, disposability, and low cost of paper-strip tests with the capability of multiplex analysis and the complex function of conventional lab-on-a-chip devices for analyte detection. Whitesides and co-workers introduced a promising concept of using a patterned paper substrate as a microfluidic platform for multiplex analyte detection.[6,7] These researchers aimed to develop simple, inexpensive, portable, disposable, and easy-to-use point-of-care platforms for developing countries and resource-limited and remote regions. To date, the primary and sparse immunoassay for the qualitative analysis of multiplex analytes on μPADs is based on a colorimetric method.[8] Unfortunately, colorimetric assays are not sufficiently sensitive or specific for accurate point-of-care use. In addition, the visual readout is usually limited to a yes/no answer, which is not adequate if the level of an analyte is critical.

Recently, there has been an emerging trend in the establishment of new analytical methods, such as electrochemical,[9,10] chemiluminescent,[11,12] and electrochemiluminescent[13] methods for the quantitative analysis of multiplex analytes on μPADs, which not only retains the features of simplicity, low cost, portability, and disposability of paper-based analytical devices but also provides new opportunities and directions for the development of precise and sensitive diagnostic devices. Nevertheless, the increasing demand for the screening of diseases at their early stage of development requires the ultrasensitive detection of biologically relevant species at an extremely low level of expression, which has inevitably led to intense research efforts on signal amplification strategies for the enhancement of detection sensitivity.[14−18] Some successful signal amplification strategies include the employment of new redox-active probes, the integration of enzyme-assisted signal amplification processes, and the incorporation of nanomaterials to increase the upload of electrochemical tags.[19−25] The last approach is particularly effective at introducing multiple redox species per binding event. To the best of our knowledge, there has been no report on the integration of signal amplification strategies into μPADs for the quantitative analysis of multiple analytes.

In this paper, for the first time, we reported the combination of signal amplification strategy with μPADs for the quantitative analysis of four kinds of cancer biomarkers as model analytes, namely, alpha-fetoprotein (AFP), carcinoembryonic antigen (CEA), cancer antigen 125 (CA125), and carbohydrate antigen

Received: May 14, 2013
Accepted: August 13, 2013
Published: August 13, 2013

   dx.doi.org/10.1021/ac401445a | *Anal. Chem.* 2013, 85, 8661−8668

153 (CA153).[26] Horseradish peroxidase (HRP) and antibody coimmobilized silica nanoparticles and graphene were used to achieve dual signal amplification. The present method showed a detection limit at the sub pg mL^{-1} level, which demonstrates the effectiveness of the strategies of signal amplification for the ultrasensitive detection of cancer biomarkers.

EXPERIMENTAL SECTION

Reagents and Materials. Human AFP, CEA, CA125, and CA153 standard solutions, mouse monoclonal capture and signal AFP, CEA, CA125, and CA153 antibodies, and HRP-labeled signal AFP, CEA, CA125, and CA153 antibodies were purchased from Meridian Life Science Inc. (TN, USA). 1-Ethyl-3-(3-dimethylaminopropyl) carbodiimide hydrochloride (EDC), *N*-hydroxysuccinimide (NHS), (3-aminopropyl)-triethoxysilane (APTS), HRP, glutaraldehyde (25% aqueous solution), chitosan, bovine serum albumin (BSA), *O*-phenylenediamine, and H_2O_2 were obtained from Sigma-Aldrich (MO, USA). A negative photoresist SU-8 3010 and developer were purchased from MicroChem Corp. (Newton, MA, USA). Carbon ink (ELECTRODEDAGPF-407C) and silver/silver chloride ink (ELECTRODAG7019 (18DB19C)) were purchased from Acheson (Germany). Whatman chromatography paper #1 (200.0 mm × 200.0 mm, pure cellulose paper) was obtained from GE Healthcare Worldwide (Pudong Shanghai, China) and used with further adjustment of the paper size. Blocking buffer for blocking the residual active sites on the antibody-immobilized paper was phosphate buffer solution (PBS), pH 7.4, containing 0.5% BSA. To minimize unspecific adsorption, the washing buffer consisted of 0.05% Tween-20 spiked into 10.0 mM PBS, pH 7.4. The 24 clinical serum samples tested in this study were provided by the Jiangsu Institute of Cancer Prevention and Cure (Nanjing, Jiangsu, China) and were analyzed at the Southeast University (Nanjing, Jiangsu, China). All of the other reagents were of analytical grade and used as received.

Apparatus. Differential pulse voltammetric (DPV) measurements and electrochemical impedance spectroscopy (EIS) were performed with a CHI 660C electrochemical workstation (CH Instrument Co., Shanghai, China). Scanning electron microscopic (SEM) images were obtained using a JEOL JSM-5510 scanning electron microscope (Japan). The UV−vis absorption spectra was recorded with a UV-3600 UV−vis-near-infrared (NIR) spectrophotometer (Shimadzu, Japan).

Fabrication of Microfluidic Paper-Based Electrochemical Immunodevice. The microfluidic paper-based electrochemical immunodevice consists of two layers of selectively patterned square filter paper of the same size (35.0 mm × 35.0 mm), as shown in Supporting Information Scheme S1. The patterned mask of this microfluidic paper-based electrochemical immunodevice was designed in two dimensions using AutoCAD2012. Paper A contains a central connecting zone (diameter = 7.0 mm) surrounded by eight working zones (diameter = 4.0 mm). Corresponding to paper A, there is one circular connecting zone (diameter = 7.0 mm) in the center of paper B. The fabrication procedure of this paper sensor is the following. Whatman chromatography paper #1 was impregnated with SU-8 3010 photoresist and then spin-coated at 2000 rpm for 30 s to spread the photoresist over the paper uniformly. The photoresist-coated paper was prebaked on a hot plate at 95 °C for 10 min. The paper was tightly covered with a predesigned film photomask and irradiated with a UV light (345 nm, 17 mw/cm^2) for 30 s. After postbaking at 95 °C for 1 min, the unpolymerized photoresist was chemically washed away by immersing the paper into acetone for 1 min and rinsing with acetone. Then, the paper was dried in a vacuum oven for 10 min and was then ready to use. The region soaked by photoresist is impermeable to liquid, whereas the photoresist-eluted region remains hydrophilic.

Eight working electrode zones were screen-printed with carbon ink in a specific area on paper A. Similarly, carbon ink and Ag/AgCl ink was screen-printed on a predesigned area of paper B as the counter electrode and the reference electrode, respectively. Finally, silver paint was applied as the conductive pads to connect the microfluidic paper-based electrochemical immunodevice to an electrochemical workstation (Supporting Information Scheme S1). Eight working electrodes share one pair of counter and reference electrodes after the two paper layers were stacked together back-to-back with four pairs of magnet (Supporting Information Scheme S2). The photoresist patterns around the electrodes on paper A and paper B constituted reservoirs of the electrochemical cells.

For paper A, the washing procedure could be performed according to the method proposed by Ge et al.[13] The working electrodes were washed by adding PBS or washing buffer to the back of the circular contacting zone while bending the paper A to an inverted-U type. Then, a piece of dry and clean blotting paper was bent to U type to contact the front side of the working electrodes on paper A. The washing buffer went through the paper and migrated along the paper channels by the capillary and gravity action to rinse the working electrodes and carried the unbound reagents into the blotting paper. This washing procedure was repeated twice by changing the bend axis, to make sure the washing was performed completely. For paper B, the washing procedure could be performed according to the method proposed by Cheng et al.[8] The paper B was washed by adding a washing buffer onto the top of the paper B while pressing the bottom against a piece of blotting paper. The washing buffer permeated paper B into the blotting paper, thereby carrying any unbound reagents with it. The washing process was important for preventing the nonspecific binding and achieving the best possible signal-to-background ratio. The printed electrodes were firmly attached to the paper surface due to the penetration of binding reagents in the ink into the paper fabric. Therefore, they would not break or peel off from the device upon washing and folding.[10]

Preparation of Nanobioprobes: The Antibody (Ab) and HRP Coimmobilized on SiO_2 Nanoparticles. We composed a panel of cancer biomarkers as model analytes: AFP, CEA, CA125, and CA153. The synthesis of monodispersed SiO_2 nanoparticles was conducted according to the reported seed-growth methods.[27,28] The TEM imaging showed that the as-prepared silica nanoparticles had a chemically clean and homogenized structure of ∼100 nm in diameter (Supporting Information Figure S1). We prepared four types of nanobioprobes: HRP and anti-AFP coimmobilized on SiO_2 nanoparticles (HRP/anti-AFP/SiO_2), HRP and anti-CEA coimmobilized on SiO_2 nanoparticles (HRP/anti-CEA/SiO_2), HRP and anti-CA125 coimmobilized on SiO_2 nanoparticles (HRP/anti-CA125/SiO_2), and HRP and anti-CA153 coimmobilized on SiO_2 nanoparticles (HRP/anti-CA153/SiO_2). The process used for the preparation of the nanobioprobes is shown in Scheme 1A; AFP was used as a model. First, 0.02 g of the silica nanospheres was dispersed in 2 mL of ethanol and treated with 0.4 mL of APTS. After stirring for 6 h, the suspension was centrifuged and washed four times with ethanol. The amino-

dx.doi.org/10.1021/ac401445a | Anal. Chem. 2013, 85, 8661−8668

Scheme 1. (A) Preparation of Nanobioprobes through the Coimmobilization of HRP and Antibody onto Monodispersed SiO_2 Nanoparticles. (B) Schematic Representation of the Fabrication and Assay Procedure Used to Prepare the Microfluidic Paper-Based Electrochemical Immunodevice[a]

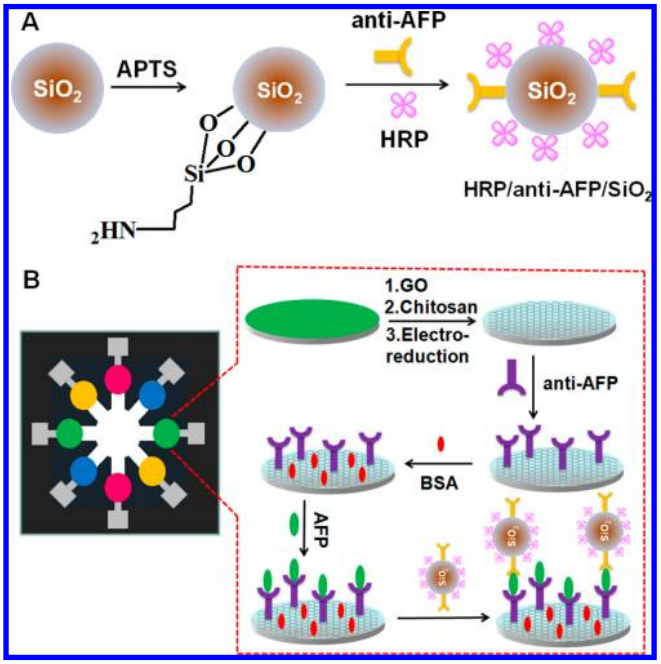

[a]AFP was provided as an example.

functionalized silica nanoparticles were then harvested. Second, the particles were incubated with 500 μL of 2.5% glutaraldehyde (in 50 mM PBS, pH 7.4) for 2 h and then washed with water. Third, the nanoparticles were redispersed in a solution of 450 μL containing 1 mg mL^{-1} HRP and 50 μL of 20 μg mL^{-1} anti-AFP. The solution was stirred at room temperature for 30 min. The unbound HRP and anti-AFP were removed by successively washing the SiO_2 nanoparticles with washing buffer. Finally, the SiO_2 nanoparticles were treated with 500 μL of blocking buffer for an additional 24 h to block any nonspecific binding site on the surface. After centrifugation and washing with washing buffer three times, the SiO_2 nanoparticles were redispersed in 1 mL of PBS, pH 7.4, and stored at 4 °C for later experiments.

Preparation of Microfluidic Paper-Based Electrochemical Immunodevice. Graphene oxide (GO) was synthesized from graphite through the modified Hummers method.[29,30] The as-synthesized graphite oxide was suspended in water and subjected to dialysis for one week to remove any residual salts. After drying at 50 °C overnight, the as-purified graphite oxide was exfoliated into GO by ultrasonicating a 0.05 wt % aqueous dispersion for 30 min. The unexfoliated graphite oxide was removed through a 5 min ultrafiltration at 2000 rcf. Then, 2 μL of 0.5 mg mL^{-1} GO solution was dropped onto each working electrode, and the electrodes were then dried in air. Then, 2 μL of 0.05% chitosan solution was dropped onto the GO film and dried in air. After the electrochemical reduction of GO at −1.0 V in PBS (pH 7.4), the modified electrode was washed with water, incubated with 2 μL of 2.5% glutaraldehyde (in 50 mM PBS, pH 7.4) for 2 h, and washed with water. Then, 2 μL of 20 μg mL^{-1} AFP, CEA, CA125, and CA153 capture antibodies was applied to the corresponding working electrodes, and they reacted at room temperature for 30 min. Subsequently, the excess antibodies were washed with washing buffer. We then blocked each working electrode by adding 2.0 μL of blocking buffer to block any possible remaining active sites against nonspecific adsorption and allowed the working electrodes to dry for 15 min under ambient conditions. After washing with washing buffer, the resulting microfluidic paper-based electrochemical immunodevice was stored at 4 °C in a dry environment prior to use.

Electrochemical Assay Procedure of the Microfluidic Paper-Based Electrochemical Immunodevice. The electrochemical assay procedures used with the prepared microfluidic paper-based electrochemical immunodevice are shown in Scheme 1B. To perform the immunoreactions and electrochemical detections, 2.0 μL of the sample solution containing different concentrations of AFP, CEA, CA125, and CA153 in PBS was added to each working electrode, allowed to incubate for 250 s at room temperature, and washed with washing buffer. Then, 2.0 μL of 10 mg mL^{-1} HRP/anti-AFP/SiO_2, HRP/anti-CEA/SiO_2, HRP/anti-CA125/SiO_2, and HRP/anti-CA153/SiO_2 was added to the corresponding working electrodes and

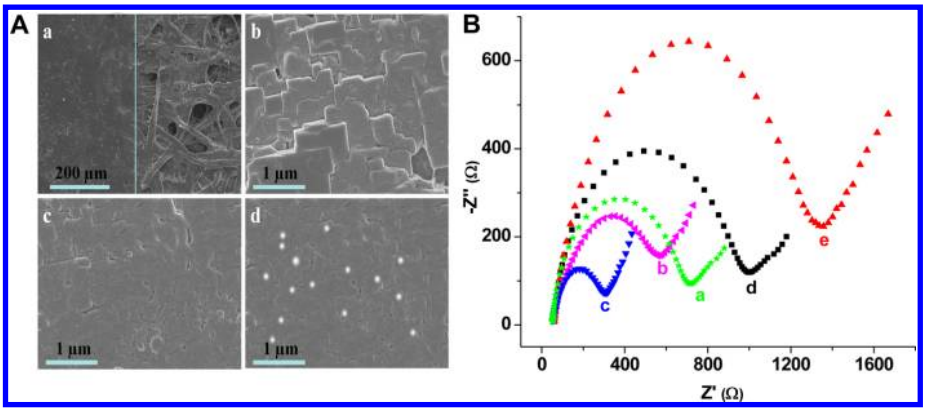

Figure 1. (A) SEM images of (a) the boundary of the photoresist pattern (left, photoresist soaked paper; right, pure paper), (b) GO/working electrode, (c) chitosan/electrochemically reduced GO/working electrode, and (d) nanobioprobes immobilized on the working electrode; the concentration of AFP is 1 ng mL^{-1}. (B) Electrochemical impedance spectroscopy (EIS) of (a) the original working electrode, (b) the GO/working electrode, (c) the chitosan/electrochemically reduced GO/working electrode (c), and the anti-AFP/glutaraldehyde/chitosan-modified working electrode (d) before and (e) after blocking with BSA in 0.1 M KCl containing 5.0 mM $[Fe(CN)_6]^{3-}$ and 5 mM $[Fe(CN)_6]^{4-}$.

dx.doi.org/10.1021/ac401445a | Anal. Chem. 2013, 85, 8661−8668

allowed to incubate for 250 s at room temperature. After that, they were washed with washing buffer and dried. For detection, 40 μL of 10.0 mM PBS buffer, pH 7.4, containing 2.0 mM *O*-phenylenediamine and 4.0 mM H_2O_2 was added to the center of the paper electrochemical cell, and the eight working electrodes were sequentially placed into the electrical circuit to trigger the electrochemical reaction. In the presence of the HRP-labeled immunocomplexes on the paper, the electroactive species 2,2′-diaminoazobenzene was first produced. The differential pulse voltammetric (DPV) measurements were then performed. To reuse this immunodevice, 50 μL of 0.1 M glycine-HCl, pH 2.2, was introduced to regenerate paper A, which was then washed twice with 50 μL of washing buffer. To ensure that the regeneration was performed completely, the regeneration procedure was repeated twice. Paper B was washed with water for recycling.

RESULTS AND DISCUSSION

Characterization of the Microfluidic Paper-Based Electrochemical Immunodevice. This immunodevice was fabricated on pure cellulose paper. The hydrophilic electrochemical cells were constructed through the selective polymerization and elution of the photoresist soaked in the paper fibers (Figure 1A-a). Therefore, the liquid conduction was limited to the hydrophilic paper channels confined by the bulk region soaked with polymerized photoresist. After the GO was coated on the surface of the working zone, a structure of crumpled sheets was generated, as shown in the SEM image (Figure 1A-b). The coating of chitosan on the electrochemically reduced GO film led to a smoother and more uniform surface topography (Figure 1A-c). When the synthesized nanobioprobes were captured on the working zone through sandwiched immunoreactions, several particles with diameters of approximately 100 nm were observed (Figure 1A-d), which indicates the successful modification of the surface of the immunodevice after each step.

The electrochemical impedance spectroscopy (EIS) of the resulting paper working zones might provide further information on the assembly process. In this work, a $[Fe(CN)_6]^{3-/4-}$ redox couple was used to characterize the immunodevice features through electrochemistry. The electron transfer of $[Fe(CN)_6]^{3-/4-}$ can be blocked by the formation of BSA/antibody/chitosan/electrochemically reduced GO composites in the paper working zone, which results in an increase in the electron transfer resistance. Figure 1B shows the Nyquist plots of EIS observed after the stepwise modification processes. The original paper working zone on the immunodevice revealed a small semicircle domain (Figure 1B, curve a), which implies a low electron transfer resistance of the redox couple. After GO was assembled on the immunodevice, the resistance decreased (Figure 1B, cure b) because the existence of the GO led to an increase in the electron transfer kinetics of $[Fe(CN)_6]^{3-/4-}$ and the effective conductive gap on the electrode/paper interface. It was observed that the chitosan-modified immunodevice exhibited a significantly lower resistance for the redox probe (Figure 1B, curve c) likely because the abundant amino groups can adsorb a significantly higher amount of the negatively charged $[Fe(CN)_6]^{3-/4-}$, which can then be easily reached at the fiber surface to accelerate electron transfer. However, the diameter of the EIS curve obtained for the antibody-modified immunodevice, which was modified through glutaraldehyde linking, increased markedly (Figure 1B, curve d) because the association of glutaraldehyde with chitosan obturated many amino groups of chitosan and formed a protein barrier for electron transfer. Similarly, BSA could also resist the electron transfer kinetics of the redox probe at the paper interface, which resulted in an increased impedance of the paper working zone (Figure 1B, curve e) and verified the immobilization of BSA.

Electrochemical Assay and Photometric Assay Using the Microfluidic Paper-Based Electrochemical Immunodevice. Using AFP as an example, the DPV responses of the anti-AFP/chitosan/electrochemically reduced GO/working electrode immobilized with nanobioprobes obtained after sandwich immunoreactions in the presence of *O*-phenylenediamine and H_2O_2 are shown in Figure 2. One DPV peak

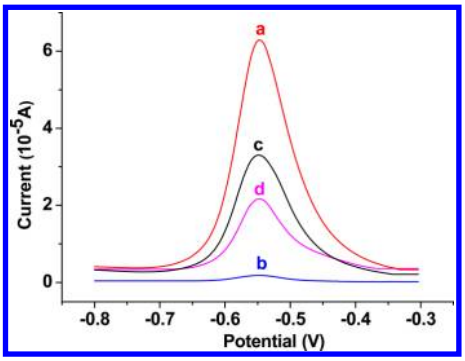

Figure 2. DPV curves obtained from (a) anti-AFP/chitosan/electrochemically reduced GO/working electrode reacted with 100 ng mL^{-1} AFP solution for 250 s and then with a nanobioprobe solution for 250 s, (b) background without antigen, (c) anti-AFP/chitosan/electrochemically reduced GO/working electrode reacted with 100 ng mL^{-1} AFP solution for 250 s and then with HRP-labeled anti-AFP solution for 250 s, and (d) anti-AFP/chitosan/working electrode reacted with 100 ng mL^{-1} AFP solution for 250 s and then with the nanobioprobe solution for 250 s.

appeared at approximately −0.548 V in the cathodic process and was generated from 2,2′-diaminoazobenzene, which was formed by the redox reaction of *O*-phenylenediamine.[31] Clearly, the captured nanobioprobes on the electrode surface led to a much higher response (Figure 2, curve a) than the nonspecific adsorption of nanobioprobes without antigen (Figure 2, curve b), which indicates a very low level of nonspecific adsorption of the nanobioprobes. To verify the silica nanoparticle-assisted signal amplification, HRP directly labeled signal antibody was used to complete the sandwich immunoreactions (Figure 2, curve c). The DPV signal was more than 2.8-fold lower than that of the electrode with the nanobioprobes. Therefore, this result confirmed the effect of the silica nanoparticle-assisted signal amplification. To verify the signal amplification of graphene, the capture antibody was directly coupled to the electrode surface through chitosan, and a comparatively lower response was obtained (Figure 2, curve d), which indicates that the presence of graphene efficiently accelerated the electron transfer and further enhanced the overall signal detected.

In addition, the bound HRP on the working electrodes can be determined by a photometric assay using tetramethyl benzidine (TMB) as the substrate.[32] When the modified working electrode was dipped into the TMB−H_2O_2 mixture solution, a large absorbance at 654 nm was observed (Supporting Information, Figure S2). The absorbance proportionally increased with the concentration of AFP in the

dx.doi.org/10.1021/ac401445a | *Anal. Chem.* 2013, 85, 8661−8668

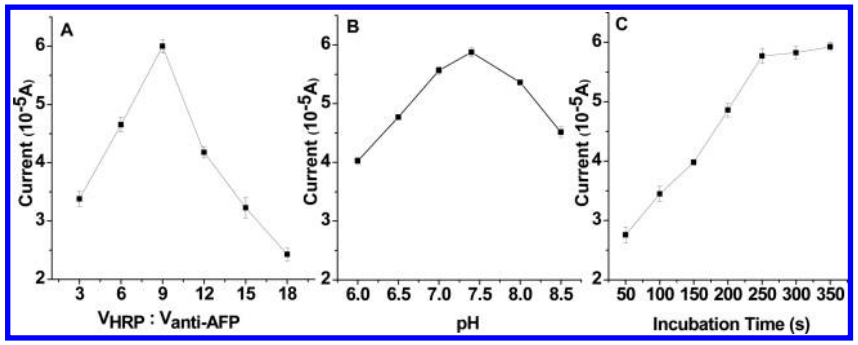

Figure 3. (A) Electrocatalytic current detected in the sandwich immunoassays as a function of the volume ratio of $V_{HRP}/V_{anti\text{-}AFP}$ during the preparation of the nanobioprobes. The concentrations of the HRP and anti-AFP were 1 mg mL^{-1} and 20 μg mL^{-1}, respectively. (B) Effect of pH on the electrocatalytic current using 100 ng mL^{-1} AFP as an example. (C) Effect of the incubation time on the electrocatalytic current using 100 ng mL^{-1} AFP as an example. Three measurements were made for each point.

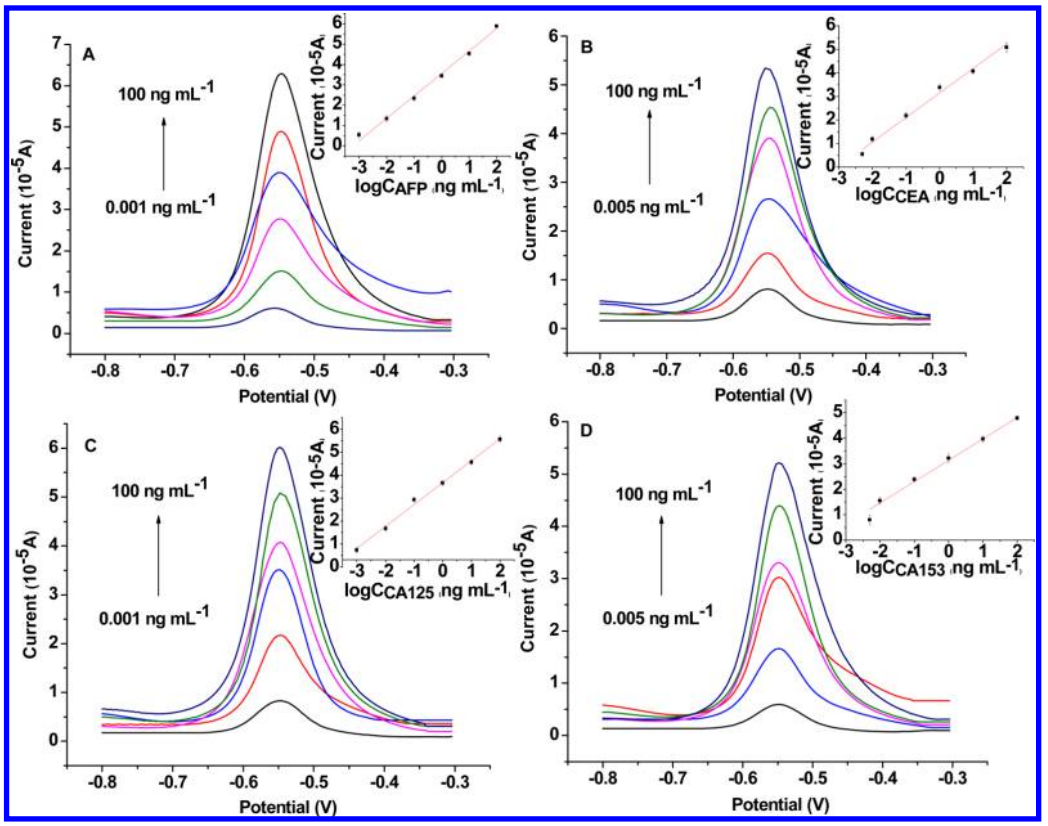

Figure 4. Plots showing the electrocatalytic currents with different concentrations of (A) AFP, (B) CEA, (C) CA125, and (D) CA153 in the incubation solutions. Inset: calibration curves for AFP, CEA, CA125, and CA153. Three measurements were made for each point.

incubation solution used for the preparation of the immunodevices, which ranged from 0.001 to 100 ng mL^{-1}, with a correlation coefficient of 0.997. All of these results demonstrate that HRP was successfully coupled to the electrode and that our proposed signal-amplification strategy is feasible.

Optimization of the Immunoassay Conditions. The detection sensitivity of the described protocol depends on the ratio of HRP and anti-AFP loaded onto the surface of the SiO_2 spheres, which is tunable during the competitive coupling reaction. Increasing the ratio of HRP in the solution could increase the absolute amount of HRP loaded per particle, which is expected to improve the signal amplified for the sandwich immunoassay. In contrast, the reduced amount of anti-AFP on the surface influences the immunocoupling efficiency to the surface-immobilized AFP. Therefore, a suitable HRP to anti-AFP ratio is necessary to produce the optimal response. As shown in Figure 3A, a volume ratio of HRP to anti-AFP of 9:1 produced the highest electrocatalytic response. A further increase in the HRP ratio resulted in reduced electrocatalytic responses.

The pH of the detection solution is another important factor in the enzymatic response. The effects of the solution pH on the DPV responses to AFP were investigated (Figure 3B). The response increased as the pH value increased from 6 to 7.4 and then decreased at pH values higher than 7.4. Thus, PBS at pH 7.4 was selected for preparing the solutions used for detection.

The incubation time is another critical parameter that affects the analytical performance and the time efficiency of the immunoassay. At room temperature, the DPV response

dx.doi.org/10.1021/ac401445a | Anal. Chem. 2013, 85, 8661−8668

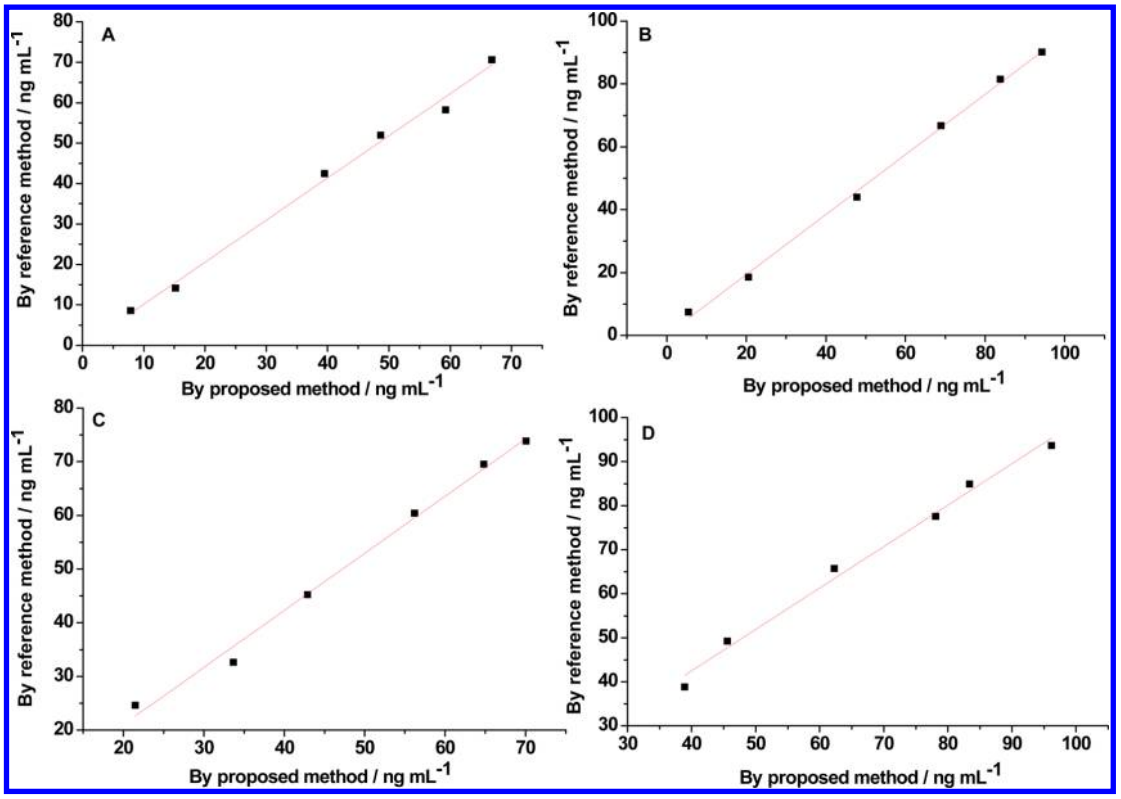

Figure 5. Correlation of the (A) AFP, (B) CEA, (C) CA125, and (D) CA153 levels in clinical human serum samples obtained using the immunodevice designed in this report.

increased with increasing incubation times in the sandwich-type immunoassays and then stabilized, which indicates the achievement of saturated binding in the immunoreaction (Figure 3C). The optimal incubation time of AFP immunocomplexes was 250 s, and accordingly, an incubation time of 250 s was selected for the subsequent experiments. The incubation process for this microfluidic paper-based electrochemical immunodevice comparatively required a much shorter incubation time than that required for traditional electrochemical immunoassays, which normally require 1−3 h of incubation at 37 °C. This difference is partly due to the high surface-to-volume ratio, the incompact porous structure, and the small volume of the graphene/chitosan-modified paper working zone. The immunoreagents need only to diffuse relatively short distances to the working electrodes to react with each other. Furthermore, as the solutions evaporate in the paper zones, the concentrations for each reagent increase, which may further enhance the binding kinetics and the formation of antibody−antigen immune complexes.[8] The short incubation time is an added advantage for the development of ultrahighly sensitive high-throughput strategies and rapid diagnostic point-of-care tests.

Analytical Performance. The analytical performance of this method was verified by applying 2.0 μL of samples of human AFP, CEA, CA125, and CA153 standard solutions at various concentrations in PBS under the above-mentioned optimized conditions. The DPV response and calibration curves for the four cancer biomarkers are shown in Figure 4. With increasing concentrations of AFP, CEA, CA125, and CA153, good correlations between the concentration of the cancer biomarkers and the DPV response were observed with similar wide dynamic ranges (0.001−100 ng mL^{-1}, 0.005−100 ng mL^{-1}, 0.001−100 ng mL^{-1}, and 0.005−100 ng mL^{-1}, respectively), which corresponded to the levels that occur naturally in human blood plasma or serum. The linear regression equations were I = 3.55 + 1.1 log (C_{AFP}/ng mL^{-1}) (R^2 = 0.9969), I = 3.14 + 1.04 log (C_{CEA}/ng mL^{-1}) (R^2 = 0.9940), I = 3.67 + 0.95 log (C_{CA125}/ng mL^{-1}) (R^2 = 0.9974), and I = 3.14 + 0.84 log (C_{CA153}/ng mL^{-1}) (R^2 = 0.9958), respectively, where I was the DPV response and C was the concentration of the cancer biomarker. The lowest detectable concentrations for the four cancer biomarkers were 0.001, 0.005, 0.001, and 0.005 ng mL^{-1}, respectively. These levels were much lower than those reported in earlier studies.[13,33−36]

We compared the levels of AFP, CEA, CA125, and CA153 in clinical human serum samples obtained using this method and with those obtained through a widely used commercially available electrochemiluminescence method at the Jiangsu Institute of Cancer Prevention and Cure. The similarity of the results between these two methods is shown in Figure 5.

Evaluation of Cross-Talk on This Microfluidic Paper-Based Electrochemical Immunodevice. An ideal electrochemical immunoarray must exclude cross-talk resulting from the diffusion of the signal reporter from one electrode to the neighboring electrodes. In our strategy, SiO_2 nanoparticles to which the antibody and HRP were coimmobilized were used as the signal reporter. On the basis of the design of the electrochemical cell in paper A (Supporting Information Scheme S1), the diffusion of the signal reporter from one electrode to its neighboring electrodes is significantly hindered by the presence of a barrier structure composed of two long highly porous paper channels. As a consequence, any potential cross-talk should be reduced to a minimum.

To further confirm the resistance to cross-talk, the cross-reactivity between the analytes and noncognate antibodies was investigated. In this microfluidic paper-based electrochemical

dx.doi.org/10.1021/ac401445a | Anal. Chem. 2013, 85, 8661−8668

immunodevice, four different capture antibodies for AFP, CA125, CA153, and CEA were immobilized separately onto eight working electrodes. The cross-reactivity was evaluated by comparing the DPV responses obtained when the device was incubated with either a blank solution or 100 ng mL^{-1} of AFP, CEA, CA125, or CA153. As expected, only the working electrode prepared with the corresponding capture antibodies yielded obvious DPV responses (Figure 6). The cross-reactivity

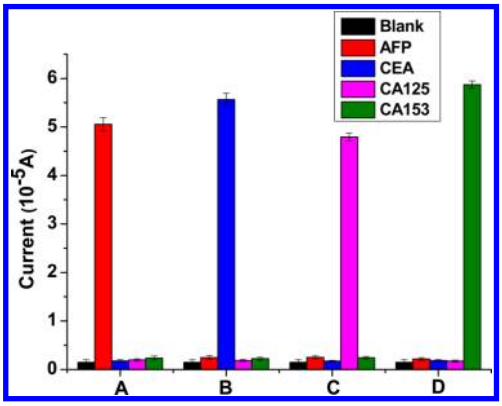

Figure 6. Cross-reactivity between the working electrodes was negligible. Electrocatalytic currents detected for the different antigens on the different electrodes: (A) anti-AFP/chitosan/electrochemically reduced GO/working electrode, (B) anti-CEA/chitosan/electrochemically reduced GO/working electrode, (C) anti-CA125/chitosan/electrochemically reduced GO/working electrode, and (D) anti-CA153/chitosan/electrochemically reduced GO/working electrode. Three measurements were made for each point.

detected between the analytes and noncognate antibodies was also negligible. In addition, as shown in Figure 2, the low nonspecific adsorption of the signal reporter with the working electrodes further indicated that the potential cross-talk between the electrodes is negligible in this microfluidic paper-based electrochemical immunodevice. Therefore, it is feasible to perform simultaneous multianalyte immunoassays with this newly designed disposable microfluidic paper-based electrochemical immunodevice.

Reproducibility, Precision, Stability, and Regeneration of Immunodevice. Using AFP as a model, the relative standard deviation (RSD) for five parallel measurements at the same working electrode on one paper immunodevice (intra-assay), incubated with the incubation solution containing 100 ng mL^{-1} AFP, was 5.8%, indicating a good precision. The detections of 100 ng mL^{-1} AFP on five different paper immunodevices fabricated independently (interassay) yielded a RSD of 6.7%, thus giving an acceptable fabrication reproducibility of the immunodevice. In addition, we also stored the dry immunodevice at 4 °C (sealed) and subsequently employed it for immunoassays at intervals of 3 days. No obvious change in the performance could be observed after the device was stored for up to 3 weeks. These results indicate that the immunodevice exhibits acceptable reliability and stability.

Lastly, the regeneration of the immunodevice was achieved by incubating it with 0.1 M glycine-HCl (pH 2.2) to dissociate the antigen−antibody complexes. Using the regeneration procedures, the microfluidic paper-based electrochemical immunodevice could be recycled at least 24 times without any obvious loss in its analytical performance. All related data were shown in Supporting Information Table S1.

CONCLUSIONS

This work is the first demonstration of the introduction of a signal amplification strategy into a simple microfluidic paper-based electrochemical immunodevice for the ultrasensitive and high-throughput detection of cancer biomarkers in a multiplex point-of-care diagnostic format. The introduction of graphene onto the surface of the immunodevice efficiently accelerated the electron transfer and enhanced the detection signal. An additional signal amplification step was achieved by reducing the physical adsorption using large silica nanoparticles as a label. As a consequence, a large amount of HRP could be introduced onto the SiO_2 nanoparticle carriers to maximize the ratio of enzyme per sandwich immunoassay. The immunodevice proposed in this work combines the simplicity and low cost of microfluidic paper-based immunodevices with the ultrasensitivity of signal amplification strategies. The newly designed immunodevice was demonstrated to be very efficient and ultrasensitive in the detection of low levels of cancer biomarkers. The advantages of this immunodevice include the following: (1) it is exceedingly inexpensive, (2) new designs can be rapidly fabricated by photolithography, (3) bulk operations of the immunoreactions on the working electrodes can be realized without compromising the stability of the reference electrode and without the counter electrode contaminating the main test solution, and (4) it is a stand-alone device that does not require external pumps or other complicated equipment to drive the fluids. These advantages make the proposed immunodevice an innately exciting platform for the design of a new generation of simple, low-cost, disposable and yet recyclable, portable point-of-care diagnostic devices. In addition to its potential clinical applications for the detection of cancer biomarkers in a high-throughput multiplex point-of-care diagnostic format, the immunodevice described in this manuscript can be easily adapted for the identification of other soluble compounds, such as enzymes and nucleic acids. Moreover, although we demonstrated the use of this applicability in immunoassays using electrochemical methods for the detection of cancer biomarkers, the immunodevice can also be modified and applied to the fields of electrochemiluminescence and photoelectrochemistry through the design of appropriate nanobioprobes with the corresponding signal antibodies.

ASSOCIATED CONTENT

Supporting Information

Schematic representation of the fabrication process of the microfluidic paper-based electrochemical immunodevice; photograph of the final ready-for-use microfluidic paper-based electrochemical immunodevice; TEM image of the as-synthesized SiO_2 nanoparticles; UV−vis absorbance spectra of HRP on the working electrodes with different AFP concentrations; experimental data for the intra-assay, the interassay precision, stability, and regeneration of the immunodevice. This material is available free of charge via the Internet at http://pubs.acs.org.

AUTHOR INFORMATION

Corresponding Authors

*E-mail: cmrhkm@nccs.com.sg. Fax: (65)-6226-3843.
*E-mail: Yuejun.Kang@ntu.edu.sg. Fax: (65)-6791-1761.

Notes

The authors declare no competing financial interest.

■ ACKNOWLEDGMENTS

This work was supported by a start-up grant from Nanyang Technological University College of Engineering, an Academic Research Fund Tier-1 from the Ministry of Education of Singapore (RG 26/11) awarded to Y.J.K., and research grants from the SingHealth Foundation, the Singapore National Medical Research Council, the Biomedical Research Council of Singapore, and the Singapore Millennium Foundation awarded to K.M.H.

■ REFERENCES

(1) Mukhopadhyay, R. *Anal. Chem.* **2009**, *81*, 8659.
(2) Martinez, A. W.; Phillips, S. T.; Whitesides, G. M. *Anal. Chem.* **2010**, *82*, 3−10.
(3) Sia, S. K.; Kricka, L. J. *Lab Chip* **2008**, *8*, 1988−1991.
(4) Whitesides, G. M. *Lab Chip* **2011**, *11*, 191−193.
(5) Mukhopadhyay, R. *Anal. Chem.* **2008**, *80*, 3949.
(6) Martinez, A. W.; Phillips, S. T.; Butte, M. J.; Whitesides, G. M. *Angew. Chem., Int. Ed.* **2007**, *46*, 1318−1320.
(7) Martinez, A. W.; Phillips, S. T.; Wiley, B. J.; Gupta, M.; Whitesides, G. M. *Lab Chip* **2008**, *8*, 2146−2150.
(8) Cheng, C. M.; Martinez, A. W.; Gong, J.; Mace, C. R.; Phillips, S. T.; Carrilho, E.; Mirica, K. A.; Whitesides, G. M. *Angew. Chem., Int. Ed.* **2010**, *49*, 4771−4774.
(9) Apilux, A.; Dungchai, W.; Siangproh, W.; Praphairaksit, N.; Henry, C. S.; Chailapakul, O. *Anal. Chem.* **2010**, *82*, 1727−1732.
(10) Nie, Z. H.; Nijhuis, C. A.; Gong, J.; Chen, X.; Kumachev, A.; Martinez, A. W; Narovlyansky, M.; Whitesides, G. M. *Lab Chip* **2010**, *10*, 477−483.
(11) Yu, J. H.; Wang, S. M.; Ge, L.; Ge, S. G. *Biosens. Bioelectron.* **2011**, *26*, 3284−3289.
(12) Yu, J. H.; Ge, L.; Huang, J. D.; Wang, S. M.; Ge, S. G. *Lab Chip* **2011**, *11*, 1286−1291.
(13) Ge, L.; Yan, J. X.; Song, X. R.; Yan, M.; Ge, S. G.; Yu, J. H. *Biomaterials* **2012**, *33*, 1024−1031.
(14) Ishii, A.; Seno, H.; Watanabe-Suzuki, K.; Kumazawa, T.; Matsushima, H.; Suzuki, O.; Katsumata, Y. *Anal. Chem.* **2000**, *72*, 404−407.
(15) Polsky, R.; Gill, R.; Kaganovsky, L.; Willner, I. *Anal. Chem.* **2006**, *78*, 2268−2271.
(16) Bao, Y. P.; Wei, T. F.; Lefebvre, P. A.; An, H.; He, L. X.; Kunkel, G. T.; Müller, U. R. *Anal. Chem.* **2006**, *78*, 2055−2059.
(17) Liu, G. D.; Wang, J.; Wu, H.; Lin, Y. *Anal. Chem.* **2006**, *78*, 7417−7423.
(18) Nam, J. M.; Thaxon, C. S.; Mirkin, C. A. *Science* **2003**, *301*, 1884−1886.
(19) Tuncagil, S.; Odaci, D.; Yildiz, E.; Timur, S.; Toppare, L. *Sens. Actuators, B* **2009**, *137*, 42−47.
(20) Chen, Z. P.; Peng, Z. F.; Luo, Y.; Qu, B.; Jiang, J. H.; Zhang, X. B.; Shen, G. L.; Yu, R. Q. *Biosens. Bioelectron.* **2007**, *23*, 485−491.
(21) Wang, J.; Meng, W. Y.; Zheng, X. F.; Liu, S. L.; Li, G. X. *Biosens. Bioelectron.* **2009**, *24*, 1598−1602.
(22) Tang, D. P.; Ren, J. J. *Anal. Chem.* **2008**, *80*, 8064−8070.
(23) Zhang, S. S.; Zhong, H.; Ding, C. F. *Anal. Chem.* **2008**, *80*, 7206−7212.
(24) Chen, L. Y.; Chen, C. L.; Li, R. N.; Li, Y.; Liu, S. Q. *Chem. Commun.* **2009**, *19*, 2670−2672.
(25) Wu, Y. F.; Chen, C. L.; Liu, S. Q. *Anal. Chem.* **2009**, *81*, 1600−1607.
(26) Li, T. X. *Modern clinical immunoassay*; Military Medical Science Press: Beijing, 2001; pp 178−209.
(27) Chang, S. M.; Lee, M.; Kim, W. S. *J. Colloid Interface Sci.* **2005**, *286*, 536−542.
(28) Lei, Z. B.; Xiao, Y.; Dang, L. Q.; Lu, M.; You, W. S. *Microporous Mesoporous Mater.* **2006**, *96*, 1−3.
(29) Li, Y. G.; Wu, Y. Y. *J. Am. Chem. Soc.* **2009**, *131*, 5851−5857.
(30) Liu, J. B.; Fu, S. H.; Yuan, B.; Li, Y. L.; Deng, Z. X. *J. Am. Chem. Soc.* **2010**, *132*, 7279−7281.
(31) Zhao, J.; Henkens, R. W.; Stonehuerner, J.; O'Daly, J. P.; Crumbliss, A. L. *J. Electroanal. Chem.* **1992**, *327*, 109−119.
(32) Liu, S. Q.; Wollenberger, U.; Halamek, J.; Leupold, E.; Stocklein, W.; Warsinke, A.; Scheller, F. W. *Chem.—Eur. J.* **2005**, *11*, 4239−4246.
(33) Wang, P. P.; Ge, L.; Yan, M.; Song, X. R.; Ge, S. G.; Yu, J. H. *Biosens. Bioelectron.* **2012**, *32*, 238−243.
(34) Wang, S. M.; Ge, L.; Song, X. R.; Yu, J. H.; Ge, S. G.; Huang, J. D.; Zeng, F. *Biosens. Bioelectron.* **2012**, *31*, 212−218.
(35) Ge, S. G.; Yu, F.; Ge, L.; Yan, M.; Yu, J. H.; Chen, D. R. *Analyst* **2012**, *137*, 4727−4733.
(36) Ge, L.; Wang, S. M.; Song, X. R.; Ge, S. G.; Yu, J. H. *Lab Chip* **2012**, *12*, 3150−3158.